Proton acceleration in the active galactic nuclei

Alexey A. Gunya*, Yakov N. Istomin**
P. N. Lebedev Physical institute in Moscow, Russia
*aagunya@lebedev.ru— — — — —**istomin@lpi.ru

Abstract

The work uses a kinetic approach. The general model is a test charged particle whose acceleration process is assumed to be without interactions. This makes it possible to estimate the limit energy that a proton can achieve when accelerated in AGN.

The centrifugal acceleration is due to the rotating poloidal magnetic field is the first step of proton acceleration occuring in the magnetosphere. Due to calculations we got conclusion that the maximum possible acceleration, γ_m, is not achieved in the magnetosphere because of the magnetic field topology nature. The naximum Lorenz factor for magnetosphere $\gamma_{magn} = \gamma_m^{2/3}$ proton achieve near the light cylinder surface Δr. The resting acceleration proton achievie in the relativistic jet. The proton reaches maximum energy when passing the total potential difference of U between the jet axis and its periphery. This voltage is created by a rotating black hole and transmitted along magnetic field lines into the jet. It is shown that the trajectories of proton in the jet are of three types: untrapped, trapped and not accelerated. Untrapped particles are not kept by poloidal and toroidal magnetic fields inside the jet, so they escape out the jet and their energy is equal to the maximum value, eU.

The obtained systems of the motion equations are solved numerically, and the output of the particular solution from them is solved analytically.

Introduction

The whole process of proton acceleration include weak pre-acceleration process in the disk, significant in the magnetosphere in the vicinity of the central machine and in the relativistic jet.

- The primary area of the proton acceleration is the disk where acceleration occurs due to turbulent accretion. The particle achieves only about 10 eV.
- In the magnetosphere particle receives energy from polar field E_θ generating due to poloidal field rotation (Blandfrod-Znajek process). The centrifugal acceleration moves particle to the light cylinder. There proton achieves general value of energy up to $E_{max}^{(2/3)} = m_p c^2 \gamma_m^{2/3}$.
- The relativistic jet is the last chain in the acceleration cycle of proton. There particle achieves maximum energy for active nucleus.

Due to procedure of dimensionless we have obtained parameters.

- Magnetization parameter (Michell like parameter) it is the ratio of rotation frequency of magnetic field lines in the magnetosphere Ω_F to nonrelativistic cyclotron frequency of particles ω_c,
$$\kappa = \Omega_F/\omega_c.$$
- Magnetic field parameter it is the ratio of toroidal magnetic field B_ϕ to the radial magnetic field B_r for the magnetosphere and to the longitudinal field B_z,
$$\alpha = B_\phi/B_r.$$
$$\alpha = B_\phi/B_z.$$
- Electric field parameter it is the ratio of multiplication of jets radius R_J and angular velocity of the the jets field Ω_F to constant of speed of light
$$\beta = R_J/R_L.$$

Here R_L is the light cylinder surface of the magnetosphere.

Magnetosphere

The central machine has magnetic field lines structure suchlike split monopole. The electromagnetic fields structure consist of poloidal magnetic field B_r, toroidal magnetic field B_ϕ and polar electric field E_θ.

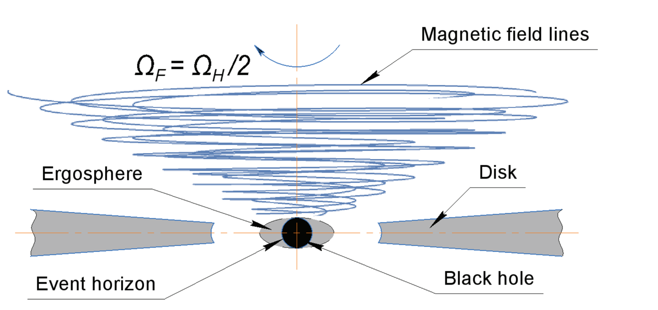

Figure 1: The magnetic field magnetosphere structure

The motion equations in spherical coordinates:

$$\begin{aligned}
&\frac{dp_r}{dt} = \frac{\kappa}{r\gamma}\left(p_\theta^2 + p_\phi^2\right) + \frac{s\alpha}{r\gamma}p_\theta,\\
&\frac{dp_\theta}{dt} = -\frac{\kappa}{r\gamma}\left(p_r p_\theta - p_\phi^2 \cot\theta\right) -\\
&-\frac{s}{r}\sin\theta + \frac{s}{r^2\gamma}p_\phi - \frac{s\alpha}{r\gamma}p_r,\\
&\frac{dp_\phi}{dt} = -\frac{\kappa}{r\gamma}\left(p_r + p_\theta \cot\theta\right)p_\phi - \frac{s}{r^2\gamma}p_\theta,\\
&\frac{dr}{dt} = \frac{\kappa}{\gamma}p_r,\\
&\frac{d\theta}{dt} = \frac{\kappa}{r\gamma}p_\theta.
\end{aligned} \tag{1}$$

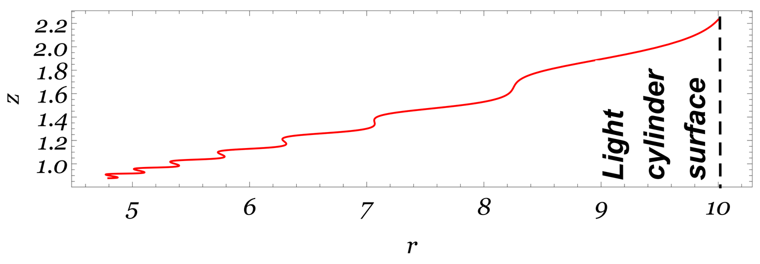

Figure 2: The $z = r \cdot cos(\Theta)$ coordinate of proton versus the radial coordinate r

The main acceleration of particles occurs near the light surface $r = 1/\sin\Theta$:

$$\Delta r = -\frac{Sign(z)\kappa\gamma_m p_r}{\sin^2\theta \quad p_\theta}|_{r=1/\sin\theta}. \tag{2}$$

In the system (1) passing from time derivatives to derivatives over coordinate r and use (2) it is obtain two cases:

- $\alpha = 0$ In this case (non AGN) magnetosphere has only poloidal field B_r with non significant toroidal field B_ϕ, so maximum value of Lorentz factor for protons doesn't exceed
$$\gamma_m = \kappa^{-1/2};$$
- $\alpha > 0$ In this case (AGN) magnetosphere has large value of toroidal field $\alpha > \kappa^{1/4}$ the maximum value of Lorentz factor for protons
$$\gamma_m = \kappa^{-2/3}.$$

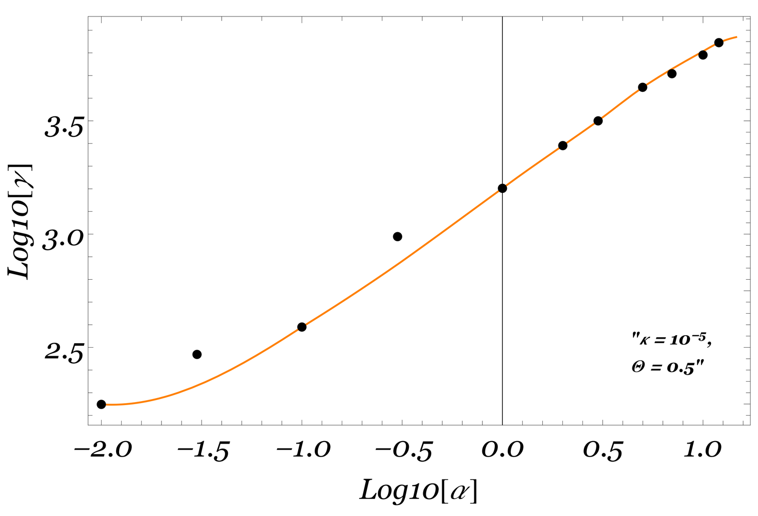

Figure 3: The Lorenz factor γ versus magnetic field parameter α

Jet

The relativistic jet is the last stage of proton acceleration, where the pre-accelerated particle can reach maximum of L-factor

$$\gamma_m = \kappa^{-1}.$$

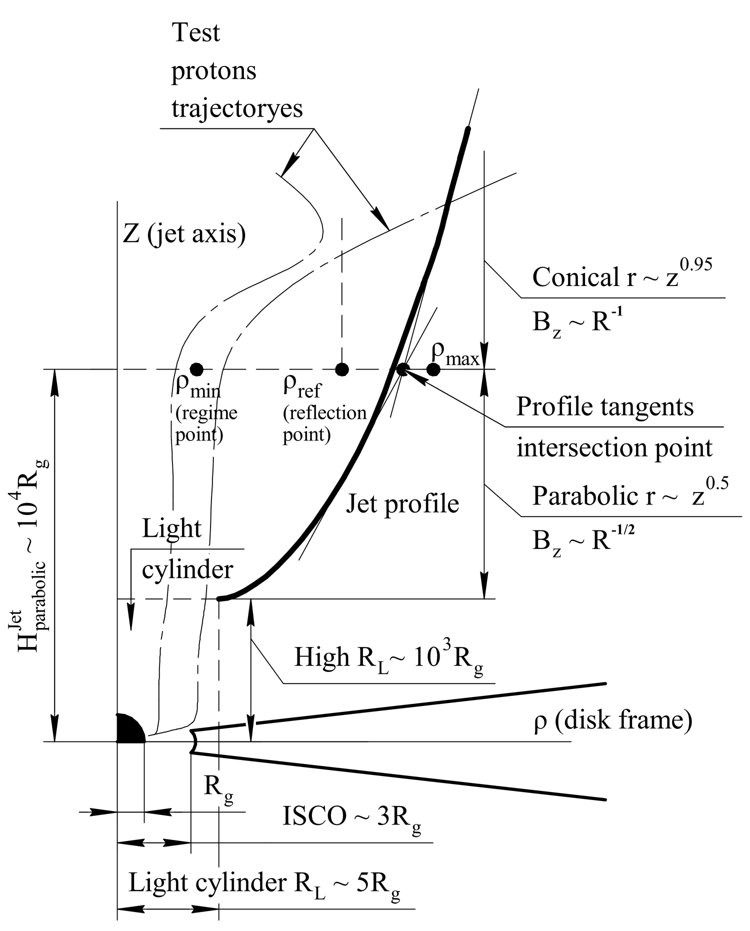

Figure 4: Relativistic jet scheme structure

$$\begin{aligned}
&\frac{dp_\rho}{dt} = \frac{p_\phi^2}{\rho\gamma} + \frac{p_\phi}{\gamma} - \alpha\frac{p_z\rho(1-\rho)^2}{\gamma} + \beta\rho(1-\rho)^2,\\
&\frac{dp_\phi}{dt} = -\frac{p_\rho p_\phi}{\rho\gamma} - \frac{p_\rho}{\gamma},\\
&\frac{dp_z}{dt} = \alpha\frac{p_\rho\rho(1-\rho)^2}{\gamma},\\
&\frac{d\rho}{dt} = \frac{p_\rho}{\gamma},\\
&\frac{d\phi}{dt} = \frac{p_\theta}{\rho\gamma},\\
&\frac{dz}{dt} = \frac{p_z}{\gamma}.
\end{aligned} \tag{3}$$

Due to calculations we got conclusions about three acceleration regimes of proton.

UNTRAPPED: $\beta^2 - \alpha^2 > a_2^2 = 36$ – protons are untrapped, they receive the maximum energy $\gamma = \gamma_m$,
TRAPPED: $19 = a_1^2 < \beta^2 - \alpha^2 < a_2^2 = 36$ – protons are trapped inside the jet, their energy oscillates around the value of $\gamma = 0.74\gamma_m$,
NO ACCELERATION: $\beta^2 - \alpha^2 < a_1^2 = 19$ – protons are not accelerated in the jet, $\gamma = \gamma_m^{2/3}$, their trajectories are pressed toward the jet axis.

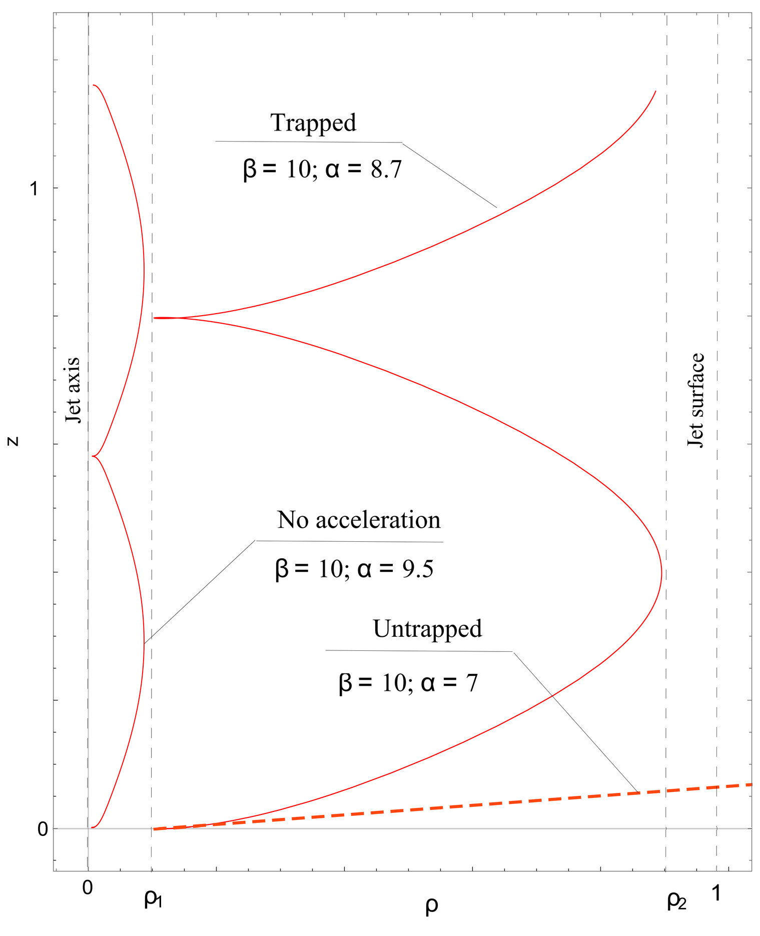

Figure 5: Particle trajectories on the plane (ρ, z). The figure shows three types of particle trajectories: untrapped, trapped and nonaccelerated.

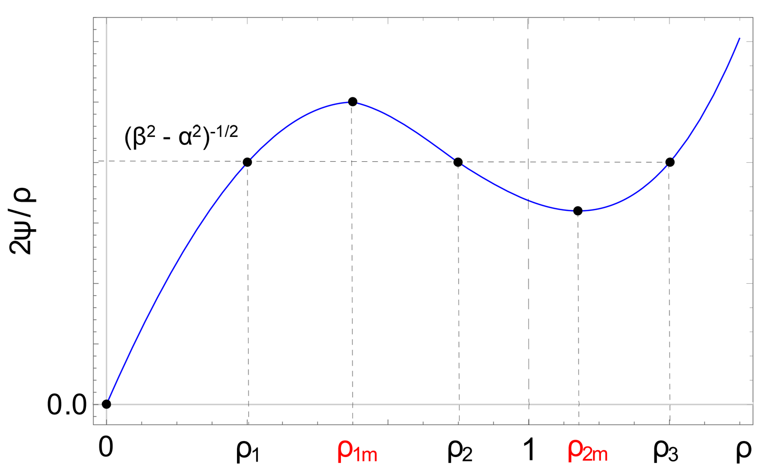

Figure 6: The reflection points of the radial motion of particles, $p_\rho = 0$, ρ_1, ρ_2, and ρ_3. The point $\rho_3 > 1$ is outside the jet. For $\beta^2 - \alpha^2 > a_2^2 = 36$, the point ρ_2 is also outside the jet, $\rho_2 > 1$, and the particle freely escapes the jet. The points ρ_{1m} and ρ_{2m} are extremes of the function $2\psi(\rho)/\rho$, $\rho_{1m} = (8 - 10^{1/2})/9 < 1$, $\rho_{2m} > 1$. At $\beta^2 - \alpha^2 < a_1^2 \simeq 19$ there are no reflection points inside the jet at all, and particle acceleration does not occur inside the jet.

Here the value of $\psi(\rho)$ is the "potential" of the radial electric field, $d\psi/d\rho = \rho(1-\rho)^2$,

$$\psi(\rho) = \frac{1}{2}\rho^2\left(1 - \frac{4}{3}\rho + \frac{1}{2}\rho^2\right). \tag{4}$$

When the difference $\beta^2 - \alpha^2$ further increases, the reflection point ρ_2 crosses the jet boundary, $\rho_2 > 1$. This means that the proton moving from the jet inner regions, crossing the jet periphery and leaves outside with receiving the maximum possible energy eU, $\gamma_m = |\beta|\psi(\rho_1) = |\beta|/12 = eU/m_pc^2$. This case exists under the condition $(\beta^2 - \alpha^2)^{-1/2} < 2\psi(\rho = 1) = 1/6$, or $\beta^2 - \alpha^2 > a_2^2 = 36$. The trajectory of such untrapped particle is shown in Fig. 6.

In the parameter range $a_1^2 < \beta^2 - \alpha^2 < a_2^2$ the particle is captured inside the jet. It oscillates between the points ρ_1 and ρ_2, changing its Lorentz factor, $12\psi(\rho_1) < \gamma/\gamma_m < 12\psi(\rho_2)$. This region of parameters is shown in Fig. 7 as the dashed area.

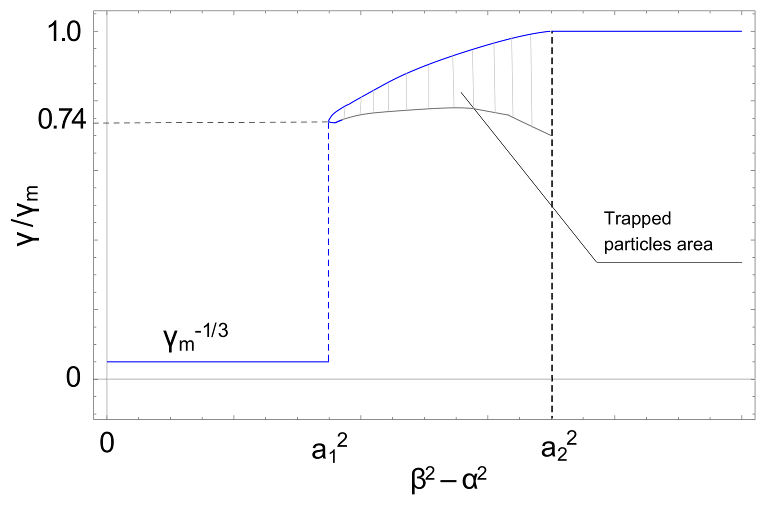

Figure 7: Lorentz factors of protons in the jet depending on the parameter $\beta^2 - \alpha^2$. At $\beta^2 - \alpha^2 > a_2^2 = 36$, the particles escape the jet and acquire the maximum energy $eU = m_pc^2\gamma_m$, $\gamma_m = \beta/12$. At $19 = a_1^2 < \beta^2 - \alpha^2 < a_2^2 = 36$ the particles are trapped in the jet, their energies oscillate around the value of the Lorentz factor of $\gamma = 0.74\gamma_m$. This region is shown as the dashed area. At $\beta^2 - \alpha^2 < a_1^2 = 19$, the particles are not accelerated in the jet and their energy equals to the energy of protons escaping the black hole magnetosphere, $\gamma = \gamma_m^{2/3} << \gamma_m$.

Black hole voltage:

$$U = 3 \cdot 10^{18} M_9 B_4 \frac{j}{1 + (1 - j^2)^{1/2}} cgs. \tag{5}$$

Axial field of the jet:

$$B_z = B_p\left(\frac{r_g}{R_J}\right)^{4/3}. \tag{6}$$

Here R_J jet radius in the intersection of the parabolic and conical profiles.

$$U_2 = B_z R_J \left\{\frac{1}{2}\left(\frac{a_2}{12}\right)^2 + \left[\frac{1}{4}\left(\frac{a_2}{12}\right)^4 + \left(\frac{8}{3}\right)^2 \frac{1}{(B_z R_J)^4}\left(\frac{L_J}{c}\right)^2\right]^{1/2}\right\}^{1/2}, a_2 = 6, \tag{7}$$

For a proton accelerated in the untrapped regime the energy is defined as,

$$E_{max}[eV] = 300 \cdot U[cgs]; \tag{8}$$

for a proton in trapped regime the average energy is,

$$E_{max}[eV] = 0.74 \cdot 300 \cdot U[cgs]; \tag{9}$$

and finally, the proton energy in the regime of motion without acceleration is,

$$E_i[eV] = 0.94GeV \cdot \left(\frac{U[eV]}{0.94GeV}\right)^{2/3}. \tag{10}$$

TABLE III. Jet parameters and acceleration regimes in the AGNs.

Object	U [cgs]	U_2 [cgs]	E_{max} [eV]	E_i [eV]	regime
OQ 530	$1.2 \cdot 10^{17}$	$3.9 \cdot 10^{17}$	$3.6 \cdot 10^{19}$	$2.4 \cdot 10^{14}$	trapped/untrapped
S5 2007+77	$1.7 \cdot 10^{17}$	$5.3 \cdot 10^{17}$	$5.1 \cdot 10^{19}$	$3.0 \cdot 10^{14}$	trapped/untrapped
S4 0954+ 5	$2.8 \cdot 10^{17}$	$9.9 \cdot 10^{17}$	$8.4 \cdot 10^{19}$	$4.2 \cdot 10^{14}$	trapped/untrapped
NGC 1275	$6.3 \cdot 10^{18}$	$2.2 \cdot 10^{18}$	$1.9 \cdot 10^{21}$	$3.3 \cdot 10^{15}$	untrapped/trapped
NGC 4261	$4.7 \cdot 10^{17}$	$1.0 \cdot 10^{17}$	$1.4 \cdot 10^{20}$	$5.9 \cdot 10^{14}$	untrapped/trapped
NGC 4486	$5.2 \cdot 10^{17}$	$1.6 \cdot 10^{17}$	$1.6 \cdot 10^{20}$	$6.4 \cdot 10^{14}$	untrapped/trapped
3C 371	$5.9 \cdot 10^{18}$	$1.5 \cdot 10^{17}$	$1.3 \cdot 10^{21}$	$3.2 \cdot 10^{15}$	untrapped
3C 405	$4.3 \cdot 10^{18}$	$6.5 \cdot 10^{17}$	$9.6 \cdot 10^{20}$	$2.6 \cdot 10^{15}$	untrapped
NGC 6251	$1.3 \cdot 10^{19}$	$4.3 \cdot 10^{17}$	$2.9 \cdot 10^{21}$	$5.5 \cdot 10^{15}$	untrapped
3C 120	$1.8 \cdot 10^{19}$	$5.6 \cdot 10^{17}$	$4.0 \cdot 10^{21}$	$6.7 \cdot 10^{15}$	untrapped
BL Lac	$4.2 \cdot 10^{19}$	$8.4 \cdot 10^{17}$	$9.3 \cdot 10^{21}$	$1.2 \cdot 10^{16}$	untrapped
3C 273	$1.8 \cdot 10^{19}$	$6.0 \cdot 10^{18}$	$5.4 \cdot 10^{21}$	$6.7 \cdot 10^{15}$	untrapped
3C 390.3	$4.4 \cdot 10^{19}$	$4.9 \cdot 10^{17}$	$9.8 \cdot 10^{21}$	$1.2 \cdot 10^{16}$	untrapped
3C 454.3	$2.7 \cdot 10^{18}$	$3.8 \cdot 10^{18}$	$8.1 \cdot 10^{20}$	$1.9 \cdot 10^{15}$	trapped/untrapped
1H 0323+342	$2.4 \cdot 10^{18}$	$7.7 \cdot 10^{17}$	$5.2 \cdot 10^{20}$	$1.7 \cdot 10^{15}$	untrapped
SS433	$3.0 \cdot 10^{18}$	$3.1 \cdot 10^{14}$	$6.7 \cdot 10^{20}$	$2.0 \cdot 10^{15}$	untrapped

References

[1] Ya. N. Istomin and A. A. Gunya, 2020, MNRAS, 492, 4, 4884–4891 - Centrifugal acceleration of protons by a supermassive black hole

[2] Ya. N. Istomin and A. A. Gunya, 2020, Phys. Rev. D 102, 043010 - Acceleration of high energy protons in AGN relativistic jets